http://dx.doi.org/10.5012/bkcs.2012.33.12.3977

Morphology Controlled Synthesis of Nanostructured Bi_2Te_3

Hee Jin Kim,[†,‡] Mi-Kyung Han,[‡,*] Ha-young Kim,[‡] Wooyoung Lee,[†,*] and Sung-Jin Kim[‡,*]

[†]*Department of Materials Science and Engineering, Yonsei University, Seoul 120-749, Korea*
[*]*E-mail: wooyoung@yonsei.ac.kr*
[‡]*Department of Chemistry and Nano Science, Ewha Womans University, Seoul 120-750, Korea*
[*]*E-mail: sjkim@ewha.ac.kr (S.-J. K.); mikihan@ewha.ac.kr (M.-K. H.)*
Received July 25, 2012, Accepted September 5, 2012

Nanostructured thermoelectric bismuth telluride (Bi_2Te_3) powders with various morphologies, such as nanoplates, nanorods, and nanotubes, were prepared by a hydrothermal method based on the reaction between $BiCl_3$, Te, and sodium ethylenediaminetetraacetate (Na_2-EDTA) at 150, 180, and 210 °C. The products were characterized by X-ray diffraction (XRD), transmission electron microscopy (TEM), high-resolution transmission electron microscopy (HRTEM), and selected area electron diffraction (SAED). The effect of reaction temperature on the morphology of the Bi_2Te_3 particles was investigated, and the possible mechanism of morphology control was proposed.

Key Words : Bi_2Te_3, Nanorod, Nanoparticle, Growth mechanism, Thermoelectric material

Introduction

Thermoelectric materials capable of the conversion of thermal into electrical energy have received considerable attention due to the potential application in various fields.[1] Materials with a large thermoelectric figure of merit, ZT, are needed to develop efficient solid-state thermoelectric devices. Recent studies have reported that low-dimensional thermoelectric materials, such as superlattices[2] and nanowires,[3] have a higher ZT due to the quantum confinement effects of charge carriers, as well as the increase of phonon scattering at the nano-scale interfaces.[4] Especially, the synthesis of nanostrucutred Bi_2Te_3 and its alloys has drawn attention due to their potential application in eco-friendly thermoelectric refrigeration near room temperature.[5] Various methods have been developed for preparing special morphologies of bismuth telluride (Bi_2Te_3), such as nanowires using pulsed electrodepostion process,[6] nanotubes using galvanic displacement process,[7] nanosheets using microwave heating process,[8] hexagonal nanoplates using solvothermal approach,[9] rod-like or flower-like nanostructures using hydrothermal method,[10] and hierarchical nanostructures using electrochemical deposition route.[11] However, it is still a challenge to develop simple and efficient synthetic methods to control the morphology of the Bi_2Te_3.

In this paper, we synthesized Bi_2Te_3 with controlled morphologies by a hydrothermal method using Na_2-EDTA as a structure directing agent. The morphologies and microstructures of nanostructured Bi_2Te_3 were studied by X-ray diffraction (XRD), transmission electron microscopy (TEM), high resolution (HR)-TEM, and selected area electron diffraction (SAED).

Experimental

Tellurium powder (6 mmol; 5 N purity), 4 mmol $BiCl_3$, and 1 g Na_2-EDTA were mixed with 60 mL water in a teflon-lined autoclave with a capacity of 100 mL. After ultrasonic agitation for 30 min, 0.8 g NaOH and 0.8 g $NaBH_4$ were added to the solution. The autoclave was then sealed, and maintained at 150, 180 and 210 °C for 24 h. During the reaction the solution was stirred by a stainless steel stirrer with a rotational speed of 200 rpm. After the reaction, the autoclave was cooled to room temperature. The black-colored product was collected by filtration, washed with deionized water and ethanol and acetone several times, and then dried at 60 °C for 12 h in a vacuum. The powder XRD patterns were collected on a Rigaku D/MAX X-ray (40 kV and 30 A) diffractometer with Cu Kα radiation (λ = 1.54056 Å). The sample morphologies, fine structures, and SAED patterns were obtained by HR-TEM using a JEOL 2100F microscope. Samples for the cross section TEM images were prepared using a Powertome ultramicrotome (RMC Products).

Results and Discussion

Figures 1(a)-1(c) depict the XRD patterns of the Bi_2Te_3 nanopowders prepared by hydrothermal synthesis at various temperatures. All the diffraction peaks in the patterns corresponded to the peaks of rhombohedral Bi_2Te_3 (JCPDS15-0863) with space group $R\bar{3}m$(166). The cell parameters calculated from the XRD pattern (a = 4.381 Å, c = 30.46 Å) were consistent with previously reported data.[12]

Figures 2-4 show the TEM images of Bi_2Te_3 samples with various morphologies prepared by the hydrothermal method using different reaction conditions. When the reaction temperature was 150 °C, Bi_2Te_3 powder with nanoplate-like morphology was formed. Figure 2(a) shows representative Bi_2Te_3 thin nanoplates with average edge lengths of 200-800 nm. The SAED pattern of a single nanoplate is shown in Figure 2(b). The hexagonal arrays of spots in the SAED

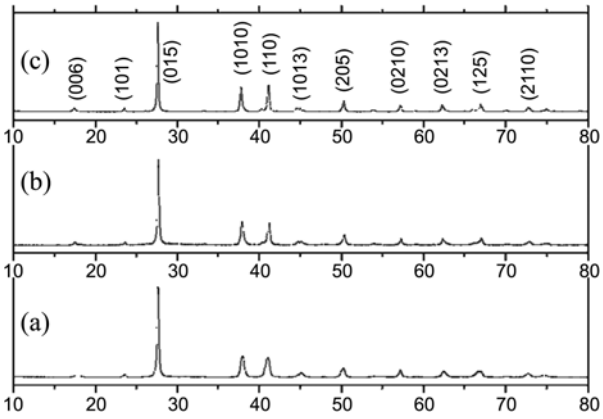

Figure 1. XRD patterns of powder products synthesized by hydrothermal method: (a) synthesized at 150 °C for 24 h, (b) synthesized at 180 °C for 24 h, and (c) synthesized at 210 °C for 24 h.

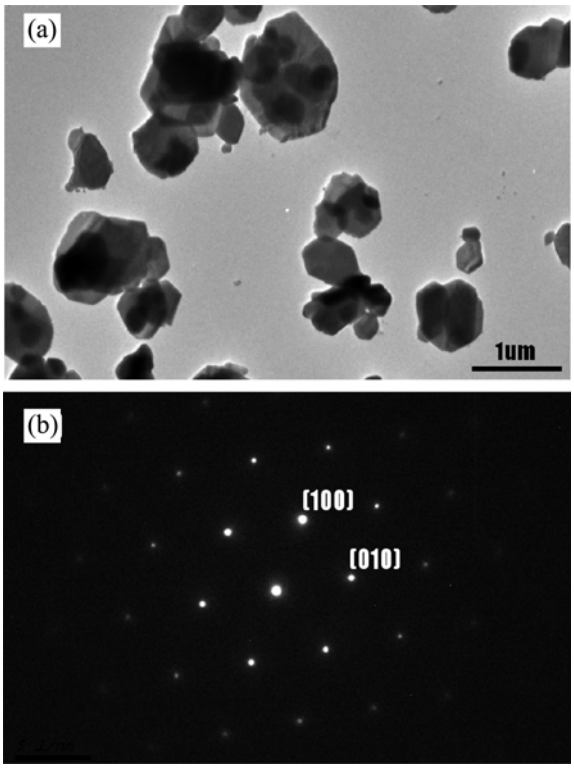

Figure 2. (a) TEM images of Bi_2Te_3 nanoplates synthesized at 150 °C for 24 h. (b) SAED pattern of nanoplates.

pattern indicate the single crystalline phase, and can be indexed based on a rhombohedral cell with lattice parameters a = 4.379 Å and c = 30.46 Å. The plane of the plate was perpendicular to the *c*-axis direction and parallel to the *ab*-planes in the Bi_2Te_3 crystal structure.

Figure 3(a) shows the TEM images of the product synthesized at 180 °C for 24 h. The morphology of the samples was nanorod-like with the diameter of 20-80 nm and over 2 μm in length. Figure 3(b) shows a representative HRTEM image and SAED pattern of the dashed square portion in Figure 3(a). From the HRTEM image of the nanorod, the distance between two neighboring faces were estimated to

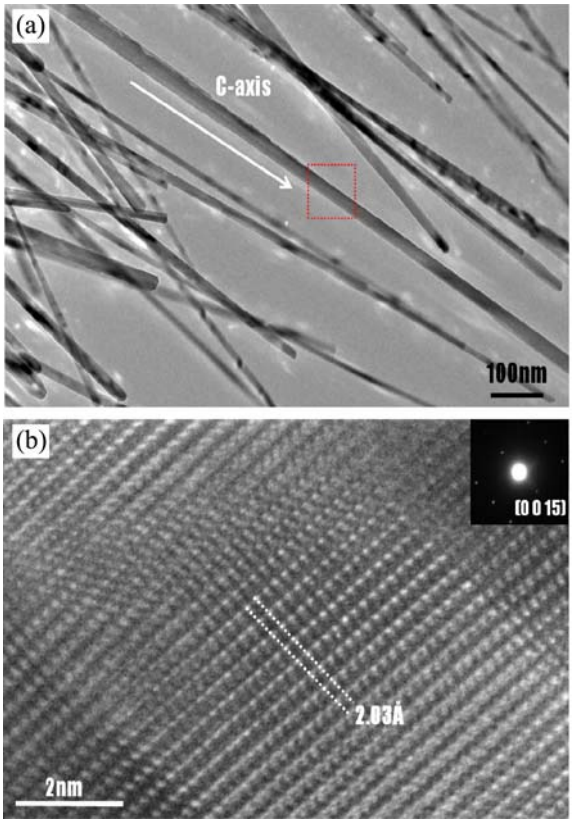

Figure 3. TEM and HRTEM images of powder product synthesized at 180 °C for 24 h. (a) TEM image of nanorod. (b) HRTEM image of the nanorod and SAED pattern (insert at upper right).

be about 2.03 Å, which was exactly same to the interplanar distance between the (0 0 15) lattice planes. Also, the SAED patterns were characteristic of single crystalline Bi_2Te_3 and indicated that the nanorods exhibited a [0 0 15] growth direction. The data was consistent with the growth of the Bi_2Te_3 nanorods along the *c*-axis of the crystal structure.

Figure 4 shows representative TEM and HRTEM images of the nanotubes synthesized at 210 °C for 24 h. Figure 4(a) shows the transparent Bi_2Te_3 nanotubes, which typically consisted of bundles of tubes with exceeding 1 μm in length and under 10 nm in diameter. The upper right inset in Figure 4(a) shows the cross sectional TEM image of bundle type Bi_2Te_3 with an internal diameter of 3-5 nm and a wall thickness of 1-3 nm. From the lattice image of the nanotube, shown in Figure 4(b), the measured distance between the two lines was approximately 5.07 Å, and the SAED pattern indexed the (0 0 6) plane, indicative of a growth direction of the Bi_2Te_3 nanotubes tilted 30° clockwise. To understand the effect of Na_2-EDTA on the growth mechanism of the nanostructured Bi_2Te_3, the same experiments were conducted under the same reaction condition but in the absence of Na_2-EDTA.

The Bi_2Te_3 nanoparticles synthesized at 150 °C for 24 h without Na_2-EDTA presented a similar morphology to the sample obtained at 150 °C for 24 h with Na_2-EDTA (Fig. 5(a)). However, the Bi_2Te_3 synthesized at 210 °C for 24 h without Na_2-EDTA displayed a different morphology from

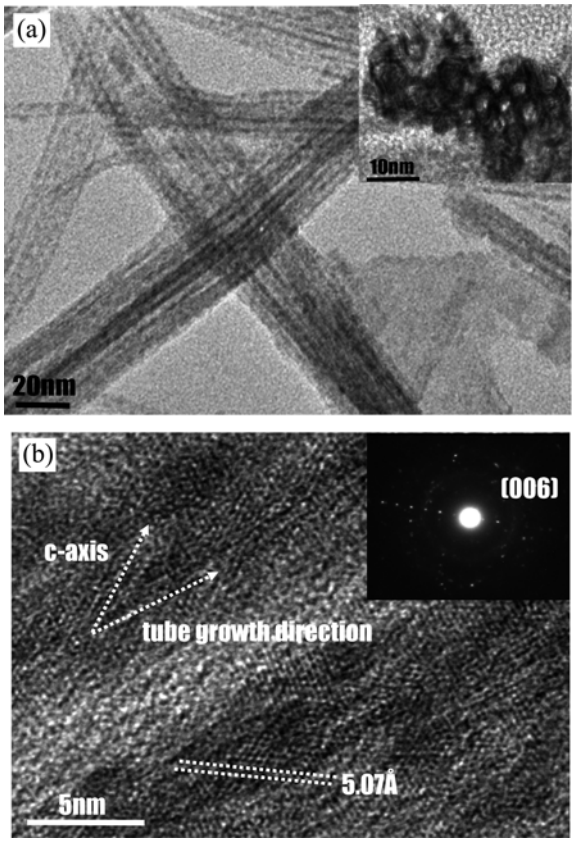

Figure 4. TEM and HRTEM images of the Bi_2Te_3 nanotube synthesized at 210 °C. (a) TEM image of the Bi_2Te_3 nanotubes; the upper right inset is the cross-sectional image of Bi_2Te_3 nanotubes. (b) HRTEM image of a Bi_2Te_3 nanotubes; the upper right inset is the SAED pattern.

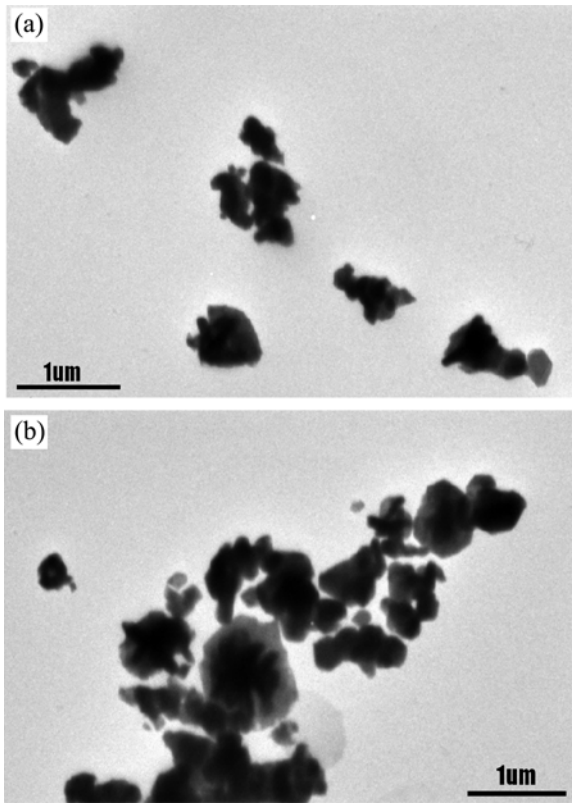

Figure 5. TEM images of the Bi_2Te_3 nanostructure synthesized without Na_2-EDTA at (a) 150 °C and (b) 210 °C.

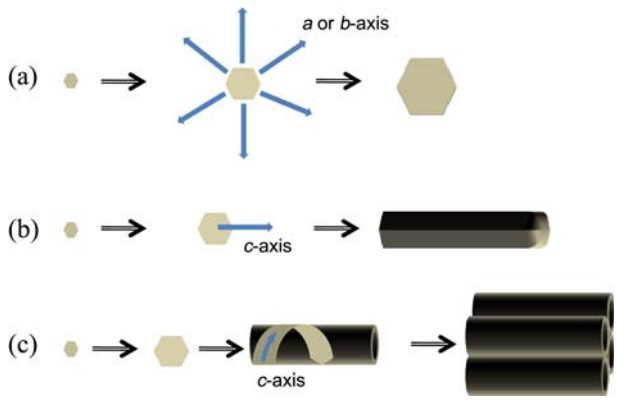

Figure 6. The schematic diagrams of the formation of Bi_2Te_3 nanostructures: (a) nanoplate, (b) nanorod, and (c) nanotube.

the sample obtained at the same condition with Na_2-EDTA (Fig. 5(b)). For both cases without Na_2-EDTA, only nanoplates were obtained. The particle sizes were typically on the order of a micron and the edges of the basal facets were not well defined. This data indicated that the presence of Na_2-EDTA was useful in controlling particle morphology and size. The possible mechanism for the formation of various Bi_2Te_3 nanostructures has been proposed.[15-17] The Bi_2Te_3 hexagonal nanoplates form due to their anisotropic crystal structural nature.[15] The repeating unit of Bi_2Te_3 structure consists of quintuple layers, Te(1)–Bi–Te(2)–Bi–Te(1), stacked perpendicular to the *c*-axis.[16] Each layer has two crystallographically different types of Te atomic sites. Te atoms in Te(2) atomic sites form covalent bondings with the six nearest Bi atoms, while Te atoms in Te(1) atomic sites are bonded to three Bi atoms by covalent bonding and three Te atoms by van der Waals bonding.[17] Te(1)-Te(1) van der Waals interaction connect the quintuple layers to form the infinite Bi_2Te_3 structure. Generally, the Bi_2Te_3 crystals grow predominantly along the *ab* plane direction because the strong covalent bonds between Bi-Te(2) can be easily extended along the plane. According to the analysis above, the reaction temperature and presence of Na_2-EDTA are important factors in the control of the morphology of Bi_2Te_3 nanostructures. The formation of bismuth telluride using the hydrothermal method can be explained as follows: Bi^{3+} ions in the solution are stabilized by the Na_2-EDTA, while Te^{2-} ions are produced from the reduction of Te by $NaBH_4$. In the solution Bi_2Te_3 are easily formed by these Bi^{3+} ions and Te^{2-} ions. During nucleation of Bi_2Te_3, the surfactant Na_2-EDTA acts as a structure directing agent, and also can induce the directional growth of nucleation to form different morphologies. Figure 6 shows a schematic diagram of the proposed formation mechanism of Bi_2Te_3 nanostructures at different temperatures. In case of low reaction temperature (about 150 °C) or reaction without Na_2-EDTA, Bi_2Te_3 crystals grow preferentially

along the *ab* plane direction with a hexagonal plate-like morphology. We observed the growth of the nanorods and nanotubes in the *c*-axis at high temperature (above 180 °C) in the presence of Na_2-EDTA. Na_2-EDTA usually binds to Bi^{3+} ions through its two amines and four carboxylates.[18] When the reaction temperature is increased to 180 °C, Bi_2Te_3 grows along the *c*-axis, instead of expending sideways along the *ab*-plane, due to the directing effect of Na_2-EDTA, speculatively caused by the capping of Bi^{3+} ions. When the reaction occurs at 210 °C, crystal growth apparently proceeded in spiral manner (Fig. 6(c)), indicating possible involvement of defects. It is suggested that some defects, such as dislocation and stacking faults, might be generated during the van der Waals stacking of crystals along the *c*-axis,[19] thereby forming nanotubes instead of the nanorods.

Conclusions

Bi_2Te_3 nanoplates, nanorods, and nanotubes are synthesized through a hydrothermal method. The reaction conditions, specifically the temperature and the stabilizing agent, plays an important role for the control of the morphology of the synthesized powders. The powder XRD measurements verified that Bi_2Te_3 nanoplates, nanorods and nanotubes are the same rhombohedral structure. The Bi_2Te_3 nanoplates grow in the *ab* plane direction at low temperature. At a temperature of 180 °C in the presence of Na_2-EDTA, Bi_2Te_3 nanorods grow along the *c*-axis direction by repeated stacking planes. At a temperature of 210 °C, the nanotubes form by stacking along a 30° tilt from the normal *c*-axis due to the formation of structural defects.

Acknowledgements. This work was supported by the Basic Science Research Program through the National Research Foundation of Korea (20110003767), Nano Material Technology Development Program through the National Research Foundation of Korea (NRF) funded by the Ministry of Education, Science and Technology (20110030147), and 'Center for Nanostructured Materials Technology' under '21st Century Frontier R&D Programs' of the Ministry of Education, Science and Technology, Korea (2011K000197).

References

1. Kanatzidis, M. G. *Chem. Mater.* **2010**, *22*, 648.
2. Venkatasubramanian, R.; Siivola, E.; Colpitts, T.; Quinn, B. O. *Nature* **2001**, *413*, 597.
3. Hochbaum, A. I.; Chen, R.; Delgado, R. D.; Liang, W.; Garnett, E. C.; Najarian, M.; Majumdar, A.; Yang, P. *Nature* **2008**, *451*, 163.
4. Hsu, K. F.; Loo, S.; Guo, F.; Chen, W.; Dyck, J. S.; Uher, C.; Hogan, T.; Polychroniadis, E. K.; Kanatzidis, M. G. *Science* **2004**, *303*, 818.
5. Hicks, L. D.; Dresselhaus, M. S. *Phys. Rev. B* **1993**, *47*, 12727.
6. Ota, J. R.; Roy, P.; Srivastava, S. K.; Popovitz-Biro, R.; Tenne, R. *Nanotechnology* **2006**, *17*, 1700.
7. Wang, W.; Zhang, G. Q.; Li, X. G. *J. Phys. Chem. C* **2008**, *112*, 15190.
8. Xiao, F.; Yoo, B.; Lee, K. H.; Myung, N. V. *J. Am. Ceram. Soc.* **2007**, *129*, 10068.
9. Jiang, Y.; Zhu, Y. J. *J. Cryst. Growth* **2007**, *306*, 351.
10. Zhang, G. Q.; Wang, W.; Lu, X. L.; Li, X. G. *Cryst. Growth Des.* **2009**, *9*, 145.
11. Salavati-Niasari, M.; Bazarganipour, M.; Davar, F. *J. Alloys Compd.* **2010**, *489*, 530.
12. JCPDS-ICDD 1997, International Centre for Diffraction Data, 12 Campus Boulevard, Newtown Square, PA 19073-3273, U.S.A.
13. Deng, Y.; Nan, C. W.; Wei, G. D.; Guo, L.; Lin, Y. H. *Chem. Phys. Lett.* **2003**, *374*, 410.
14. Lu, W. G.; Ding, Y.; Chen, Y. X.; Wang, Z. L.; Fang, J. Y. *J. Am. Chem. Soc.* **2005**, *127*, 10112.
15. Deng, Y.; Nan, C.-W.; Wei, G.-D.; Guo, L.; Lin, Y.-H. *Chem. Phys. Lett.* **2003**, *374*, 410.
16. Zhao, X. B.; Ji, X. H.; Zhang, Y. H.; Cao, G. S.; Tu, J. P. *Appl. Phys. A* **2005**, *80*, 1567.
17. Fan, X. A.; Yang, J. Y.; Xie, Z.; Li, K.; Zhu, W.; Duan, X. K.; Xiao, C. J.; Zhang, Q. Q. *J. Phys. D: Appl. Phys.* **2007**, *40*, 5975.
18. Kirchner, S. B. *Inorganic Syntheses* **1957**, *5*, 186.
19. Wang, Z.; Wang, F.-Q.; Chen, H.; Zhu, L.; Yu, H.-J.; Jian, X.-Y. *J. Alloys Compd.* **2010**, *492*, 50.